On the Factors Influencing the Performance of Solar Reactors for Water Disinfection with Photosensitized Singlet Oxygen

ARTICLE *in* ENVIRONMENTAL SCIENCE AND TECHNOLOGY · FEBRUARY 2008

Impact Factor: 5.33 · DOI: 10.1021/es071762y · Source: PubMed

4 AUTHORS, INCLUDING:

David García-Fresnadillo
Complutense University of Madrid
27 PUBLICATIONS **530** CITATIONS
SEE PROFILE

Guillermo Orellana
Complutense University of Madrid
126 PUBLICATIONS **1,904** CITATIONS
SEE PROFILE

On the Factors Influencing the Performance of Solar Reactors for Water Disinfection with Photosensitized Singlet Oxygen

FRANCISCO MANJÓN, LAURA VILLÉN, DAVID GARCÍA-FRESNADILLO, AND GUILLERMO ORELLANA*

Laboratory of Applied Photochemistry, Department of Organic Chemistry, Faculty of Chemistry, Universidad Complutense de Madrid, E-28040 Madrid, Spain

Received July 17, 2006. Revised manuscript received October 11, 2007. Accepted October 16, 2007.

Two solar reactors based on compound parabolic collectors (CPCs) were optimized for water disinfection by photosensitized singlet oxygen ($^1O_2$) production in the heterogeneous phase. Sensitizing materials containing Ru(II) complexes immobilized on porous silicone were produced, photochemically characterized, and successfully tested for the inactivation of up to 10^4 CFU mL^{-1} of waterborne *Escherichia coli* (gram-negative) or *Enterococcus faecalis* (gram-positive) bacteria. The main factors determining the performance of the solar reactors are the type of photosensitizing material, the sensitizer loading, the CPC collector geometry (fin- vs coaxial-type), the fluid rheology, and the balance between concurrent photothermal−photolytic and $^1O_2$ effects on the microorganisms' inactivation. In this way, at the 40° N latitude of Spain, water can be disinfected on a sunny day (0.6–0.8 MJ m^{-2} L^{-1} accumulated solar radiation dose in the 360–700 nm range, typically 5–6 h of sunlight) with a fin-type reactor containing 0.6 m^2 of photosensitizing material saturated with tris(4,7-diphenyl-1,10-phenanthroline)ruthenium(II) (ca. 2.0 g m^{-2}). The optimum rheological conditions require laminar-to-transitional water flow in both prototypes. The fin-type system showed better inactivation efficiency than the coaxial reactor due to a more important photolytic contribution. The durability of the sensitizing materials was tested and the operational lifetime of the photocatalyst is at least three months without any reduction in the bacteria inactivation efficiency. Solar water disinfection with $^1O_2$-generating films is demonstrated to be an effective technique for use in isolated regions of developing countries with high yearly average sunshine.

1. Introduction

Water is a primary need for human beings. The availability of drinking water is a critical problem for an important part of the world population, mainly located in third-world countries where over 1 billion people suffer diseases related to waterborne microorganisms (*1*). Classical water disinfection techniques such as chlorination, and less-common alternatives based on other oxidizing reagents (ozone, chlorine dioxide, etc.) or physical treatments (membrane filtration or UV-C illumination), are typically used in urban or industrial areas (*2, 3*). However, they are difficult to apply in isolated regions, especially those in poorer countries, due to the lack of infrastructures.

The so-called solar disinfection (SODIS) method (*4*) is a cheaper alternative to obtain pathogen-free water in those countries situated in the solar radiation belt. Such a water disinfection method uses the combined effect of the UV-A component of sunlight plus an infrared-powered temperature increase to inactivate bacteria. However, the technique requires plastic bottles (1–2.5 L), limiting the total amount of water treated per day, is not equally effective with all types of bacteria or turbid waters (NTU > 30), and requires appropriate weather conditions.

Reactive oxygen species (ROS) such as the hydroxyl radical ($HO^\bullet$), singlet oxygen ($^1O_2$), or superoxide anion ($O_2^{\bullet-}$) are powerful oxidants able to react with most organic molecules and, consequently, to damage microorganisms. Therefore, the use of ROS is a promising alternative for water disinfection (*5, 6*). These oxidizing species can be readily generated in water from dissolved oxygen by homogeneous or heterogeneous photocatalysis and sunlight, without the need for additional chemicals other than the light-absorbing catalyst. In the case of a homogeneous process, an additional step involving photocatalyst removal is required, while if supported dyes are used, this is an unnecessary process (*6*).

Hydroxyl radicals, commonly photogenerated using titanium dioxide (TiO_2) and UV-A radiation have been employed in water disinfection and decontamination processes (*7–13*). Singlet oxygen, $O_2(^1\Delta_g)$, the lowest electronic excited state of molecular oxygen, might be promising in photodisinfection processes since all known types of microorganisms undergo $^1O_2$-induced damage in their membrane lipids, proteins, or genes (*14*). $^1O_2$ generation by photosensitization can be performed on laboratory and industrial scales. This process requires a sensitizer dye that, upon the absorption of light, transfers the energy excess of the excited state to O_2, yielding $^1O_2$ (see Scheme 1 in the Supporting Information) (*15*). $^1O_2$ sensitizers such as methylene blue, rose bengal, or porphyrins have shown remarkable disinfection efficiency in homogeneous media (*16, 17*). However, they have mainly been applied in the environmental field to the photooxidation of waterborne polluting dyes (*18, 19*), rather than to drinking water disinfection (*20, 21*). Compared to the hydroxyl radical, singlet oxygen displays advantages when used for water disinfection: (i) $^1O_2$ is a more selective oxidant; (ii) 1–2 orders of magnitude lower sensitizer loadings are required than with supported TiO_2, which makes costs comparable; (iii) the photogeneration of $HO^\bullet$ with TiO_2 requires UV-A radiation, while $^1O_2$ can be produced with both UV and visible light, making better use of the solar spectrum (*9–13, 20, 22*).

Ru(II) coordination complexes display a number of advantages over purely organic sensitizers, such as their broad and strong absorption band in the visible spectrum ($\varepsilon_{max} > 10^4$ M^{-1} cm^{-1}), intersystem crossing quantum yields close to unity, long excited-state lifetimes (in the μs range), significant $^1O_2$ production quantum yields (0.2–1.0 in solution), good thermal and photochemical stability, and the possibility of immobilizing them on a suitable substrate by adequate selection or functionalization of their ligands (*21, 23–27*).

The design of solar reactors for water disinfection based on heterogeneous photocatalysis relies on solar thermal collectors adapted to carry out a photochemical process (*9*). In this regard, compound parabolic collectors (CPCs) have proved to be an optimal choice for photochemical applica-

* Corresponding author phone: 34-91-3944220; fax: 34-91-3944103; e-mail: orellana@quim.ucm.es.

TABLE 1. Photophysical Characterization of the Photosensitizing Materials

material	$\tau_{M_0}/\mu s^a$	$\tau_M/\mu s^{a,b}$	$P_{O_2}^T(\tau_M)^{b,c}$	$P_{O_2}^T(I)^{b,d}$	$\tau_\Delta/\mu s^e$	$\Phi_{\Delta op}{}^a$
RDP^{2+}/pSil	3.1	0.48	0.84 ± 0.02	0.85 ± 0.07	40	2.0×10^{-3}
RDB^{2+}/pSil	0.75	0.27	0.64 ± 0.04	0.56 ± 0.06	45	0.8×10^{-3}

[a] Uncertainty: ±10%. [b] Air-equilibrated water. [c] From time-resolved emission measurements. [d] From steady-state emission measurements. [e] Uncertainty: ±15%.

tions, as these devices offer some of the advantages displayed by parabolic trough collectors (PTCs) and those of nonconcentrating reactors (*9, 28, 29*). PTC technology focuses sunlight but requires a tracking system to maximize the direct incident radiation, while nonconcentrating reactors use static flat plates with a suitable tilt but do not take advantage of the global daily solar irradiation. However, tilted static CPC collectors, typically used in thermal applications such as solar water heating or the solar desalination of water (*30*), allow collection of all the global incident sunlight thanks to a reflective surface optimized under the principles of nonimaging optics.

In this paper, we have identified the role played by different parameters influencing water photodisinfection with $^1O_2$ generated by sunlight using two different sensitizing materials and two prototypes of CPC-based reactors.

2. Experimental Section

2.1. Materials and Instrumentation. *2.1.a. Preparation of the Sensitizing Dyes.* The selected $^1O_2$ photosensitizers were [tris(4,7-diphenyl-1,10-phenanthroline)ruthenium(II)] dichloride and [tris(4,4′-diphenyl-2,2-bipyridine)ruthenium(II)] dihexafluorophosphate, abbreviated RDP^{2+} and RDB^{2+}, respectively. RDP^{2+} was prepared from the appropriate commercial chelating ligand and $RuCl_3$ hydrate according to an established procedure (*24*). RDB^{2+} was synthesized and characterized as described in the Supporting Information.

2.1.b. Preparation of Silicone Strips with Photosensitizer. RDP^{2+} and RDB^{2+} were immobilized by hydrophobic interactions onto porous poly(dimethylsiloxane) films (CulturSil, Cellon, Luxembourg). This material, abbreviated pSil, consists of a single-sided 0.5-mm-thick porous silicone layer on a $1500 \times 35 \times 1$ mm strip of nonporous silicone. The pSil strips were dyed following a reported procedure (*31*) from RDP^{2+} stock solutions (3×10^{-5}, 1.3×10^{-4}, and 7.0×10^{-4} M, in 1:9 v/v MeOH/water). Photosensitizing materials with 0.85, 1.97, and 2.0 g m^{-2} (±10%) loading, respectively, were obtained, as deduced from a spectrophotometric analysis of the supernatants plus washouts (*31*). RDB^{2+} was immobilized at a 1.5 g m^{-2} level following a similar procedure (Supporting Information). The photochemical characterization of the $^1O_2$ photosensitizing materials is described in the Supporting Information.

2.2. Solar Reactors. Two different configurations, namely, coaxial- and fin-type, based on CPC technology (AoSol, Portugal, under license of Ecosystem Environmental Services, Spain) were tested. The solar CPC reactors comprised 1500 × 50 mm (46 mm i.d.) borosilicate glass tubes, had 1 m^2 of collector area each, and differed only in the optimized light collectors (five W-shaped or seven U-shaped section units, respectively, Figure S1, Supporting Information) and in the corresponding geometry of the photosensitizing material support (a 1500×32 mm polypropylene coaxial cylinder or a $1500 \times 41 \times 6$ mm rectangular prism, respectively) (*31, 32*). To study the water flow effects on bacteria disinfection rates, two different centrifugal pumps were used (PanWorld, Japan, 12-W NH-10PX-H and 100-W NH-50PX-X models, supplying a maximum of 2 and 15 L min^{-1}, respectively). When changes in water flow rates were required, the recirculating valve to the tank was adjusted to carry out the corresponding experiment. A general layout of the systems is depicted in Figure S1 (Supporting Information).

2.3. Working Conditions. Taking into account the successful results of the disinfection experiments carried out with a solar-simulated laboratory-scale photoreactor (*21*), the working conditions were scaled up to the solar reactors. The following parameters were considered: total water volume to be treated (V), illuminated area of the photosensitizing material (A), water flow rate (q_V), and incident solar irradiance (E). The values of each one of the selected parameters were as close as possible for both photoreactor prototypes in order to determine the configuration providing the highest microorganism inactivation efficiency.

2.4. Solar Disinfection Assays. To compare the bacteria inactivation efficiencies of RDP^{2+}/pSil and RDB^{2+}/pSil, preliminary experiments were performed with both materials in the solar-simulated laboratory reactor. The microorganism strains used to evaluate the effect of the photogenerated $^1O_2$ on the disinfection efficiency were *Escherichia coli* (CECT 4624) and *Enterococcus faecalis* (CECT 5143), two representative types of gram-negative and gram-positive bacteria, respectively. Initial microorganism concentrations of 10^2 and 10^4 CFU mL^{-1} in innoculated mineral water were tested in the CPCs with a typical continuous illumination of 5 h of sunlight exposure per assay. The bacteria culturing, procedures, and evaluation of results (Supporting Information) are similar to those described (*31*), unless stated otherwise.

2.5. Measurement of the Solar Radiation Dose. The accumulated dose of incident sunlight at 40° N latitude in the 360–760 nm spectral region was measured with a fiber-optic spectroradiometer as described in the Supporting Information, after calibration using the ASTM G-173 reference solar spectrum of AM-1 irradiance at 37° N latitude (*33*). The measurement uncertainty was below 10% (*34*).

2.6. Operational $^1O_2$ Production Quantum Yield ($\Phi_{\Delta op}$). This parameter was estimated by chemical scavenging of the $^1O_2$ photogenerated by the sensitizing material immersed in water, following the method of Verlhac et al. (*35*) (Supporting Information).

2.7. Durability of the Polymer-Supported Ru(II) Photosensitizers. Pieces of the photocatalytic materials were periodically cut out from the solar reactors in order to evaluate their aging due to sunlight illumination. Emission lifetimes, reflectance, and emission spectra were measured on those materials at different irradiation intervals (Supporting Information).

3. Results

3.1. Characterization of the Photosensitizing Materials. The normalized absorption, reflectance, and emission spectra of RDP^{2+}/pSil in the visible spectrum are shown in Figure S2 (Supporting Information). Table 1 summarizes the preexponentially weighted luminescence lifetimes of the photosensitizing materials in N_2-purged or air-equilibrated water, the probability of sensitizer excited-state quenching by oxygen under air-equilibrated conditions ($P_{O_2}^T$), the measured $^1O_2$ emission lifetime, and the operational $^1O_2$ production quantum yield. A typical time-drive experiment to determine

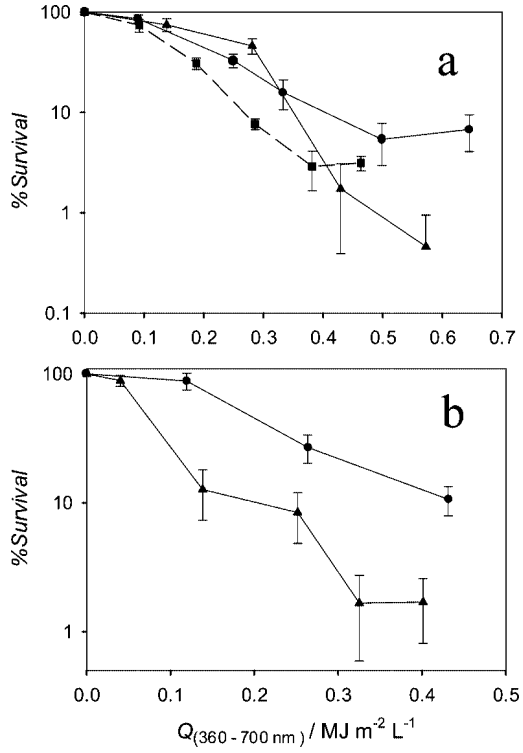

FIGURE 1. Influence of rheology on 10^4 CFU mL^{-1} *E. coli* inactivation in the solar reactors. (a) Effect of the water flow rate in the coaxial prototype with the accumulated radiation dose (*Q*): 0.25 L min^{-1} (circles), 2 L min^{-1} (triangles), and 15 L min^{-1} (squares). (b) Inactivation under the same rheological conditions: coaxial (circles, 1.1 L min^{-1}) and fin (triangles, 2 L min^{-1}) types.

$P_{O_2}{}^T$ for the RDP^{2+}/pSil material from steady-state emission measurements is shown in Figure S3 (Supporting Information).

The observed emission kinetics of the supported photosensitizer in the presence and absence of O_2 is complex, so that a sum of 2–3 exponentials was used to fit the experimental profile (Figure S4, Supporting Information, depicts a typical luminescence decay trace of the polymer-supported RDP^{2+} sensitizer). The production of $^1O_2$ by the immobilized photosensitizers has been evidenced by its characteristic NIR luminescence centered at 1270 nm (*15*). Figure S5 (Supporting Information) displays the emission decay of singlet oxygen photogenerated by RDP^{2+}/pSil.

3.2. Disinfection Assays. Preliminary inactivation experiments with a laboratory-scale reactor and both types of photocatalysts are depicted in Figure S6 (Supporting Information). On the basis of these results, we carried out inactivation tests with our two solar reactor prototypes. In order to select the rheological conditions in the reactors, *E. coli* disinfection tests were performed at different water flow rates with the coaxial prototype (Figure 1a), and also with the two photoreactors under different flow rates but the same rheological conditions (Figure 1b). Subsequent inactivation assays with *E. faecalis* at initial concentrations of 10^2 and 10^4 CFU mL^{-1} using RDP^{2+}/pSil were also run to compare both prototypes from the viewpoint of inactivation efficiency (Figure 2). As control experiments, the evolution of *E. coli* and *E. faecalis* concentrations at the two initial levels tested (10^2 and 10^4 CFU mL^{-1}) using undyed pSil strips under sunlight are depicted in Figure 3a and b, respectively.

3.3. Durability of the Photosensitizing Material. Changes in the absorption, reflectance, and emission of light of the photosensitizing materials were observed as a consequence of the solar disinfection assays. No changes were observed in their $P_{O_2}{}^T$ and emission lifetimes of the immobilized dye. However, the normalized emission intensity decreased with the accumulated radiation dose (Figure S7, Supporting Information). A hypochromic shift in the reflectance of the RDP^{2+}/pSil material was also detected, although efficient microorganism inactivation was observed until the last disinfection assay was performed, without noticeable changes in the bacteria inactivation kinetics.

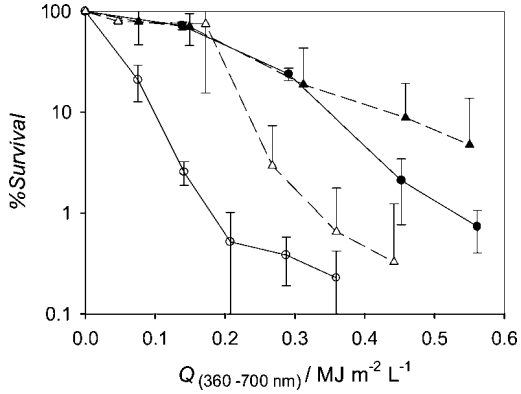

FIGURE 2. Inactivation of 10^2 (triangles, dashed lines) and 10^4 CFU (circles, solid lines) mL^{-1} *E. faecalis* with RDP^{2+}/pSil in the coaxial- (black symbols) and fin- (open symbols) type prototypes; flow rate = 2 L min^{-1}.

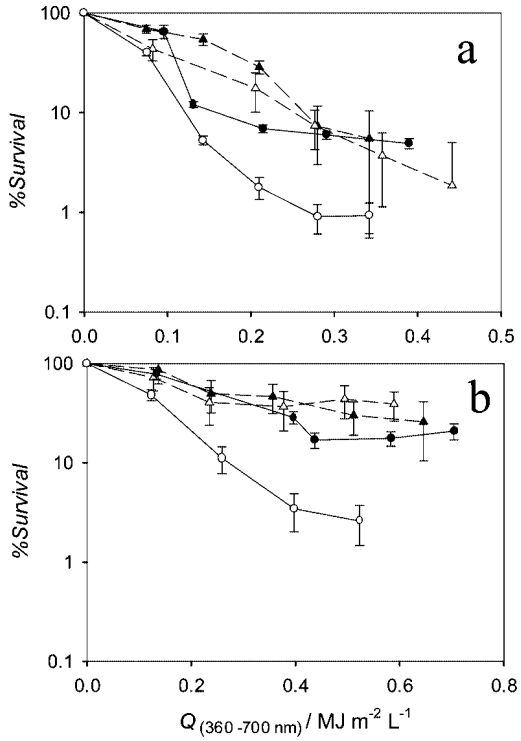

FIGURE 3. Bacteria inactivation with blank pSil strips with the prototypes: (a) fin type and (b) coaxial reactor. Initial concentrations: 10^2 CFU mL^{-1} (triangles, dashed lines) and 10^4 CFU mL^{-1} (circles, solid lines) of *E. faecalis* (open symbols) and *E. coli* (black symbols); flow rate = 2 L min^{-1}.

4. Discussion

To rationalize the discussion, we have divided this section into two parts, namely, the photosensitizing materials themselves and the working parameters influencing the water disinfection efficiency of the solar reactors.

4.1. Photosensitizing Material-Related Parameters. *4.1.a. Sensitizer Nature.* Typical organic $^1O_2$ sensitizers such as rose bengal or methylene blue and (metallo)porphyrins have demonstrated good water disinfection efficiency in the

homogeneous phase. However, with these sensitizers, photobleaching occurs quickly (around 100% of the sensitizer is degraded after 2 h under sunlight) (*16, 17*) so that photostability must be investigated.

Ru(II) complexes with polyazaheterocyclic chelating ligands strongly absorb in the 400–550 nm region, and when the ligands bear phenyl substituents, they become efficient $^1O_2$ photosensitizers (*24*). In particular, those synthesized from 4,7-diphenyl-1,10-phenanthroline, such as RDP^{2+}, display high $^1O_2$ production quantum yields (0.97 and 0.42 in MeOH and in water, respectively) (*24*). Moreover, ligand photodechelation has been demonstrated to be a very inefficient process in Ru(II) polypyridyls, with a quantum yield of 3×10^{-4} (*36*). Photodechelation does not necessarily lead to degradation, particularly in rigid ligands such as 1,10-phenanthroline (phen).

The photodegradation of Ru(II) dyes in solution and immobilized onto different polymers has been reported and mainly attributed to oxidation by the photogenerated $^1O_2$ (*37–40*). This process is minimized when the Ru(II) coordination sphere contains 2,2′-bipyridine ligands, due to the lack of the ethylenic bridge of phen derivatives that is mainly responsible for their reactivity with $^1O_2$ (*40*). Unfortunately, bipyridine complexes show a higher photosubstitution quantum yield due to the free rotation around the pyridine–pyridine bond once the Ru−N bond breaks down in the triplet (nonluminescent) metal-centered excited state (*41*). Ru(II) complexes based on 2,2′-bipyridine derivatives are also fairly good $^1O_2$ photosensitizers (for instance, Φ_Δ 0.73 and 0.22 for tris(2,2′-bipyridine)ruthenium(II) in MeOH and in water, respectively) (*24*). Therefore we selected RDP^{2+} and RDB^{2+} as benchmark sensitizers to test the balance between efficient $^1O_2$ production and photobleaching.

Since no dissolved sensitizer must be present in the water after the disinfection treatment, it is mandatory for practical purposes to immobilize the dye on an adequate polymer support. Hydrophobic Ru(II) complexes can be strongly and reproducibly immobilized by adsorption onto polymer materials such as porous silicone (*21, 31*) without noticeable leaching ($<10^{-9}$ M sublethal levels have been measured by photon-counting luminescence measurements).

4.1.b. Polymer Support and Sensitizer Loading. In a previous work, we explored the suitability of several Ru(II) $^1O_2$ photosensitizers embedded into different polymer supports for microorganism inactivation (*21*). Silicone rubbers display a number of advantages for $^1O_2$ production, namely, extremely high oxygen permeability (*42*), and the photogenerated $^1O_2$ exhibits a 10-fold lifetime in these polymers (ca. 40 μs) compared to water (*21*). Furthermore, porous silicone is optically translucent, mechanically robust, significantly photostable, and chemically inert, and the commercially available material we have selected shows excellent interaction with microorganisms (*43*). Therefore, different RDP^{2+} loadings on pSil were tested.

At RDP^{2+} initial concentrations above 1.3×10^{-4} M in MeOH/water (1:9 v/v), the resulting loading on the porous material is close to its saturation limit (once repeated washings to remove the weakly bound sensitizer were performed). This result is supported by data obtained from loading procedures carried out at different initial concentrations of the sensitizer: Preparations from 3×10^{-5} M RDP^{2+} yielded a 0.85 g m^{-2} doped material, while 1.3×10^{-4} M dye produced a silicone with 1.97 g m^{-2} loading (2.3-fold factor). However, experiments carried out with a sensitizer concentration close to its solubility limit in the MeOH/water mixture (7.0×10^{-4} M) yielded a 2.0 g m^{-2} loading. This maximum sensitizer load was used throughout for the bacteria inactivation tests, as high dye levels are advantageous if photobleaching occurs. Similarly, saturation of the polymer with ca. 1.5 g m^{-2} of RDB^{2+} was achieved using a 2.6×10^{-4} M stock solution of the sensitizer in MeOH/water (1:4 v/v).

4.1.c. Photochemical Parameters of the Sensitizing Materials. The probability of oxygen quenching of the photoexcited sensitizer ($P_{O_2}^T$) was determined from steady-state intensity (I) and lifetime (τ_M) emission measurements using eqs 1 and 2, where the subscript "0" refers to an absence of oxygen.

$$P_O{}^T = 1 - \frac{I}{I_0} \quad (1)$$

$$P_O{}^T = 1 - \frac{\tau_M}{\tau_M} \quad (2)$$

Both photocatalysts are efficiently deactivated by O_2 ($P_{O_2}^T$, ca. 0.85 and 0.60 for the immobilized RDP^{2+} and RDB^{2+}, respectively, independently of the dye loading, Table 1). However, the quenching probability is higher for the RDP^{2+} sensitizer, according to its longer excited-state lifetime (τ_{M0}). Singlet oxygen formation within the silicone has been evidenced from its lifetime (42 ± 5 μs) in the wet materials (Figure S5, Supporting Information). This value is significantly longer than the 4.4 μs measured in water (*44*), regardless of the sensitizer dye.

We have determined also the *operational* $^1O_2$ production quantum yield ($\Phi_{\Delta op}$, namely, from the amount of $^1O_2$ trapped by the scavenging solution where the photosensitizing material is immersed) after making all the necessary corrections for (i) the incident light, (ii) the absorbance of the *N*,*N*-dimethyl-*p*-nitrosoaniline (RNO) indicator (*35*), and (iii) the decrease in the RNO concentration due to its photodegradation and adsorption onto the polymer material, and considering that 12 $^1O_2$ molecules are required for bleaching just one indicator dye molecule (*35*). From the operational standpoint (Table 1), RDP^{2+}/pSil is ca. 3-fold more efficient than RDB^{2+}/pSil. This result can be attributed to the lower $P_{O_2}^T$ of RDB^{2+} and to its higher hydrophobicity due to its PF_6^- counterions, which would allow this sensitizer to enter the inner hydrophobic domains of the polymer support, limiting the escape of the generated $^1O_2$. Therefore, the RDP^{2+}/pSil system would be the best choice for photosensitized $^1O_2$ production (without considering its photostability). The experimental results displayed in Figure S6 (Supporting Information) show however that both photosensitizing materials behave similarly from the point of view of the bacteria inactivation efficiency. These results might be explained if much more $^1O_2$ is generated than the actual amount required for the microorganism inactivation.

4.1.d. Endurance of the Sensitizing Materials. The effect of the accumulated radiation on the stability to light of the photocatalysts was evaluated from their luminescence intensity. The latter decreased with the radiation dose due to sensitizer photobleaching (Figure S7, Supporting Information). Both Ru(II) complexes loaded to saturation on pSil showed a similar behavior: after an initial steep decrease, a plateau was reached at ca. 20 MJ m^{-2} (about 15 h of sunlight exposure or three disinfection experiments). The strongest decrease was observed with RDP^{2+}/pSil (its initial emission is reduced to 20% at 20 MJ m^{-2}, while it decreases to 50% for RDB^{2+}/pSil at the same accumulated dose), demonstrating the lower photostability of RDP^{2+} because of its structural features discussed above. Nevertheless, equally efficient bacteria inactivation was still observed at the maximal accumulated radiation dose tested so far for the RDP^{2+}/pSil material (ca. 500 MJ m^{-2}). Therefore, we can conclude that both photosensitizing materials display similar bacteria inactivation efficiencies, as RDP^{2+}/pSil has a 3-fold larger Φ_Δ but poorer photostability while RDB^{2+}/pSil exhibits the opposite features. An additional advantage, regardless of the system used and since degradation of the pSil support was never observed, is that the polymer strips could eventually

TABLE 2. Working Parameters (Water Volume, Illuminated Area, Flow Rate, and Irradiance) in the Water Disinfection Experiments Using RDP^{2+}/pSil Photosensitizing Material in the CPC Solar Reactors

reactor	V/L[a]	A/m^2	q_V/L min^{-1}	E/W m^{-2}[b]
coaxial-type	10	0.57[c]	2.0	400
fin-type	17.5	0.65[d]	2.0	400
factor[e]	0.57	0.88	1	1

[a] Treated volume of water per experiment. [b] W m^{-2} (360–700 nm). [c] Four tubes (out of five) with photocatalyst strips, ca. 0.8 m^2 of illuminated collector area. [d] Five tubes (out of seven) with photocatalyst strips, ca. 0.8 m^2 of illuminated collector area. [e] Proportionality factor between the parameters of the coaxial-/fin-type reactors.

be reloaded with photosensitizer and reused in new water disinfection treatments.

4.2. Reactors and Their Operational Parameters. *4.2.a. Solar Collector Configuration.* The two different CPCs described in Section 2.2 were designed by the manufacturer to collect all the incident solar radiation by mirrors of optimized geometry according to the receiver shape (cylindrical or rectangular prismatic). However, their identical reflective surface (1 m^2) mandates that the two systems contain a different number of glass tubes (five in the coaxial- and seven in the fin-type reactor), so that different areas of photosensitizing material are illuminated. As it is expected that the larger the *illuminated area* of dyed film, the more efficient the inactivation of bacteria, the photosensitizer area is an important factor to be considered. Therefore, to be able to compare the performance of the two solar reactors from the point of view of $^1O_2$ photogeneration, the area of sensitizing material was kept as constant as feasible (ca. 0.6 m^2) for both prototypes. This was achieved by using a different number of fully coated inner supports in each reactor (four tubes in the coaxial- and five in the fin-type, which corresponds to ca. 0.75 m^2 of the collector area; Table 2).

Taking into account that the different configurations of the coaxial- and fin-type collectors determine different shapes for the photocatalyst framework and, consequently, a different water volume per tube, the *total water volume* is another factor which is difficult to match. The water volume per glass tube of the fin-type configuration is ca. 2 L, while it is only 1 L in the coaxial geometry; consequently, the total water volume in each reactor has to be different (10 L in the coaxial- and 17.5 L in the fin-type).

As is shown in Figure 1b and Figure 2, the fin-type system always yields faster bacteria inactivation. Therefore, factors other than just the photosensitizer area must determine the efficiency of bacteria inactivation, such as the *rheological regime*, which is directly related to the *water flow*, and the *illuminated water volume per tube*.

The effect of the *rheological regime* (characterized by the Reynolds number, Re) was checked by selecting three different water flow rates, namely, 0.25, 2, and 15 L min^{-1}, corresponding to laminar (Re $\sim$ 500), transitional (Re $\sim$ 4000), and turbulent conditions (Re $\sim$ 30 000), respectively (Figure 1a). In spite of a slower initial inactivation rate, the best results were obtained with the intermediate flow, as at lower flow rates the required number of water cycles for bacteria inactivation would be too large for the limited daily sunlight hours; additionally, the exchange of microorganisms between the photosensitizing material surface (where $^1O_2$ effect actually occurs) and the aqueous phase is not favored. At higher flow rates, the contact time between the microorganisms and the polymer surface is lowered.

Taking into account that 2 L min^{-1} provided the best results and to guarantee reproducibility, the pump supplying this maximum flow was finally selected for further disinfection tests with both solar reactors. Such working flow corresponds to a laminar-to-transitional regime in the fin-type reactor (Re $\sim$ 2100), while it is a transitional regime in the coaxial one (Re $\sim$ 4000). When the flow conditions were modified to operate both reactors with a similar Re number (2.0 and 1.1 L min^{-1} in the fin- and coaxial-type, respectively, Re $\sim$ 2100), the fin-based reactor yielded 1 order of magnitude higher microorganism inactivation than the coaxial prototype for the same accumulated radiation dose (0.4 MJ m^{-2} L^{-1}, Figure 1b). If the same flow rate is used in both reactors (2 L min^{-1}), 1 order of magnitude higher inactivation was also achieved with the fin-type collector for the same solar dose of 0.4 MJ m^{-2} L^{-1} (Figure 2). Therefore, the optimum working conditions for both reactors that allow an efficient interaction between bacteria and the photosensitizing material and consequently the best inactivation results seem to be laminar-to-transitional rheology.

Once it has been demonstrated that, under comparable rheological conditions, the fin-type reactor displays a better performance, we address whether this difference might be attributed to the effect of the *illuminated water volume per tube*. Considering that the distinct collector configurations determine different optical pathlengths, direct solar disinfection (photolytic effect) should be considered. The photolytic effect can be evaluated from Figure 3a and b, depicting experiments carried out with both reactors operated at the selected working conditions but with blank pSil strips (no $^1O_2$ production). In the coaxial collector, where the illuminated volume per tube is ca. 1 L, a 50% decrease in the survival of initial bacteria is observed except for the highly $^1O_2$-sensitive gram-positive *E. faecalis* (a 50-fold decrease has been measured at a high initial concentration). On the other hand, the fin-type collector, with ca. 2 L of illuminated water per tube, shows a 1–2 log decrease regardless of the microorganism tested and its initial level. These results confirm that two processes are responsible for the observed bacteria inactivation: the photolytic and $^1O_2$ effects.

A simple attempt to discern both contributions would require subtracting the effect of the blank from the total inactivation; however, the result would not be realistic as the photosensitizing material is orange-colored while the white appearance of the undyed support causes significant diffuse reflection. Therefore, the contribution of the photolytic effect would be overestimated with such an approach. This is confirmed by previous results (*31*) where only a 10% inactivation of waterborne bacteria was observed by using just the (gray) inner polypropylene framework that normally holds the photosensitizing strips in place. Although it is difficult to separate both contributions, similar inactivation trends with the photolytic plus $^1O_2$ (Figure 2) and the photolytic effect alone (Figure 3a) are observed on *E. faecalis* with the fin-type reactor. Therefore, the photolytic effect plays an important role but is the effect of $^1O_2$ on bacteria survival, which determines whether disinfection can be reached or not for a particular solar dose. In the case of the coaxial reactor, Figures 2 and 3b do not show the same behavior at different initial bacteria concentrations, suggesting that the photolytic effect is less important than $^1O_2$ inactivation (see below in Section 4.ii.c). This fact can be attributed to the smaller illuminated volume in the coaxial collector. The same conclusions can also be drawn for *E. coli* (*31*).

Strains from culture collections, rather than from the natural environment, were used in our study. While this is probably enough for comparing the performance of the two collector designs and the different photosensitizing materials, it might overestimate the efficiency of the solar reactors for treating natural waters. Enteric bacteria strains from culture collections could be more susceptible to solar inactivation

than naturally ocurring bacteria, partially due to a loss of environmental resistance due to repeated passaging (*45*).

4.2.b. Water Temperature Effect. The temperature reached inside the solar collectors during the disinfection tests varied between 25 and 50 °C depending on the insolation. Experiments above 50 °C were discarded to avoid deviations due to heat effects. Control runs in the absence of photosensitizing material or blank polymer showed that the combined effect of sunlight and temperature accounts for ca. 10% of *E. faecalis* and *E. coli* inactivation (*31*). No significant differences in the water temperature reached during the treatment were observed between the fin- and the coaxial-type collector configurations (Figure S8, Supporting Information).

4.2.c. Operation Time. A time span of ca. 5 h for the disinfection experiments was employed. After the solar treatment, the *E. faecalis* survival is always lower than 10% of the initial concentration (Figure 2) and a similar outcome was observed with *E. coli* (*31*). These results may be significantly improved with longer irradiation times or in those areas with a higher solar radiation dose than that of our experiments. This operation time is comparable to or better than that required by alternative techniques such as SODIS (typically 6 h for disinfection in semiarid regions) (*4*) or TiO_2-supported photocatalysis (approximately 2 h for a 2 log decrease of 10^4 CFU mL^{-1} *E. coli* bacteria) (*13*).

Moreover, the faster inactivation rate of the 10^4 CFU mL^{-1} suspension (Figure 2), particularly evident for the fin-type reactor, may be attributed to the heterogeneous nature of the $^1O_2$ production together with the short lifetime of such species (vide supra). Only the silicone-bound bacteria will be attacked by $^1O_2$, and the binding kinetics are strongly dependent on the waterborne microorganism concentration.

4.2.d. Accumulated Radiation. The higher the accumulated radiation, the lower the bacteria survival (Figures 1−3). With our fin-type setup for an accumulated radiation dose in the 0.6–0.8 MJ m^{-2} L^{-1} range (in the 360–700 nm region), a complete loss of bacteria culturability is observed with waters containing 10^2 or 10^4 CFU mL^{-1} initial concentrations of *E. coli* or *E. faecalis*. On sunny days at 40° N latitude, the mean irradiance is ca. 400 W m^{-2} in the 360–700 nm region. Therefore, treatment periods of 5–6 h are equivalent to a total solar dose of ca. 1.75 MJ m^{-2} L^{-1}. In contrast, the UVA-based SODIS process requires ca. 5 MJ m^{-2} L^{-1} of total solar dose for complete microorganism disinfection (estimated from data available in ref *4*).

Field tests of the $^1O_2$ photosensitizing materials containing Ru(II)−polyazaheterocyclic complexes adsorbed on porous silicone have demonstrated to be promising photocatalysts for solar water disinfection treatments in less-developed regions of semiarid countries (*46*). The cost-effectiveness of the more efficient sensitizer-based treatment versus the photolytic sunlight-only systems can be judged from the ca. $20 (USD) price tag of the photoreactive dye per reactor used in our study.

Acknowledgments

The authors thank the European Union for INCO grants (ICA4-CT-2002-10001, "SOLWATER", and ICA3-CT-2002-10028, "AQUACAT") and the Spanish Ministry of Education and Science (grant CTQ2006-15610-C02-01_BQU) for supporting this project and S. Enriquez and J. Montero from the Spanish National Institute for Meteorology for providing the solar radiation data. We acknowledge collaboration in some experiments of Dr. M. E. Jiménez-Hernández, M. L. Contreras, and Y. Almonacid. F. M. thanks Complutense University of Madrid for a doctoral grant.

Supporting Information Available

Additional experimental and results details and additional figures (Figures S1−S8). This material is available free of charge via the Internet at http://pubs.acs.org.

Literature Cited

(1) Jaffe, S. Facing the Global Water Crisis. *The Scientist* **2004**, *18*, 18–22.
(2) Najm, I.; Trusell, R. R. New and Emerging Drinking Water Treatment Technologies. *Identifying Future Drinking Water Contaminants*; National Academy Press: Washington, DC, 1998; pp 220–243.
(3) Hrubec, J. *Quality of Drinking Water*; Springer: Berlin, 1998; Vol. 2.
(4) Solar Water Disinfection. http://www.sodis.ch (accessed Oct 2007).
(5) Kruk, I. The Handbook of Environmental Chemistry *Reactions and Processes, Part I: Environmental Toxicology and Chemistry of Oxygen Species*; Hutzinger, O., Ed.; Springer: Berlin, 1998; Vol. 2.
(6) Larson, R. A.; Weber, E. J. *Reaction Mechanisms in Environmental Organic Chemistry*; CRC Press: Boca Raton, FL, 1994.
(7) Wiszniowski, J.; Robert, D.; Surmacz-Gorska, J.; Miksch, K.; Malato, S.; Weber, J. V. Solar Photocatalytic Degradation of Humic Acids as a Model of Organic Compounds of Landfill Leachate in Pilot Plant Experiments: Influence of Inorganic Salts. *Appl. Catal., B* **2004**, *53*, 127–137.
(8) Guillard, C.; Disdier, J.; Monnet, C.; Dussaud, J.; Malato, S.; Blanco, J.; Maldonado, M. I.; Herrmann, J. M. Solar Efficiency of a New Deposited Titania Photocatalyst: Chlorophenol, Pesticide and Dye Removal Applications. *Appl. Catal., B* **2003**, *46*, 319–332.
(9) McLoughlin, O. A.; Kehoe, S. C.; McGuigan, K. G.; Duffy, E. F.; Touati, F. A.; Gernjak, W.; Alberola, I. O.; Malato, S.; Gill, L. W. Solar Disinfection of Contaminated Water: a Comparison of Three Small-Scale Reactors. *Solar Energy* **2004**, *77*, 657–664.
(10) Salih, F. M. Enhancement of Solar Inactivation of Escherichia coli by Titanium Dioxide Photocatalytic Oxidation. *J. Appl. Microbiol.* **2002**, *92*, 920–926.
(11) Rincón, A. G.; Pulgarín, C. Photocatalytical Inactivation of E. coli: Effect of (Continuous-Intermittent) Light Intensity and of (Suspended-Fixed) TiO_2 Concentration. *Appl. Catal., B.* **2003**, *44*, 263–284.
(12) Watts, R. J.; Kong, S.; Orr, M. P.; Miller, G. C.; Henry, B. E. Photocatalytic Inactivation of Coliform Bacteria and Viruses in Secondary Wastewater Effluent. *Water Res.* **1995**, *29*, 95–100.
(13) Fernández, P.; Blanco, J.; Sichel, C.; Malato, S. Water Disinfection by Solar Photocatalysis Using Compound Parabolic Collectors. *Catal. Today* **2005**, *101*, 345–352.
(14) Hamblin, M. R.; Hasan, T. Photodynamic Therapy: A new Antimicrobial Approach to Infectious Disease. *Photochem. Photobiol. Sci.* **2004**, *3*, 436–450.
(15) Schweitzer, C.; Schmidt, R. Physical Mechanisms of Generation and Deactivation of Singlet Oxygen. *Chem. Rev.* **2003**, *103*, 1685–1757.
(16) Cooper, A. T.; Goswami, D. Y. Evaluation of Methylene Blue and Rose Bengal for Dye Sensitized Solar Water Treatment. *J. Solar Energy Eng.* **2002**, *124*, 305–310.
(17) Jemli, M.; Alouini, Z.; Sabbahi, S.; Gueddari, M. Destruction of Fecal Bacteria in Wastewater by Three Photosensitizers. *J. Environ. Monit.* **2002**, *4*, 511–516.
(18) Gryglik, D.; Miller, J. S.; Ledakowicz, S. Solar Energy Utilization in Degradation of 2-Chlorophenol by Immobilized Photosensitizers. *Solar Energy* **2004**, *77*, 615–623.
(19) Karapire, C.; Kus, M.; Turkmen, G.; Trevithick-Sutton, C. C.; Foote, C. S.; Icli, S. Photooxidation Studies with Perylenediimides in Solution, PVC and Sol-Gel Thin Films under Concentrated Sun Light. *Solar Energy* **2005**, *78*, 5–17.
(20) Yokoi, H.; Shiragami, T.; Hirose, J.; Kawauchi, T.; Hinoue, K.; Fueda, Y.; Nobuhara, K.; Akazaki, I.; Yasuda, M. Bactericidal Effect of a Silica Gel-Supported Porphyrinatoantimony(V) Complex under Visible Light Irradiation. *World J. Microbiol. Biotechnol.* **2003**, *19*, 559–563.
(21) Jiménez-Hernández, M. E.; Manjón, F.; García-Fresnadillo, D.; Orellana, G. Solar Water Disinfection by Oxygen Photogenerated with Polymer-Supported Ru(II) Sensitizer. *Solar Energy* **2006**, *80*, 1382–1387.
(22) Rengifo-Herrera, J. A.; Sanabria, J.; Machuca, F.; Dierolf, C. F.; Pulgarin, C.; Orellana, G. A Comparison of Solar Photocatalytic Inactivation of Waterborne E. coli Using Tris(2,2′-bipyridine)ruthenium(II), Rose Bengal and TiO_2. *J. Solar Energy Eng.* **2007**, *129*, 135–140.
(23) Demas, J. N.; DeGraff, B. A. Design and Applications of Highly Luminescent Transition Metal Complexes. *Anal. Chem.* **1991**, *63*, 829–837.

(24) García-Fresnadillo, D.; Georgiadou, Y.; Orellana, G.; Braun, A. M.; Oliveros, E. Singlet-Oxygen ($^1\Delta_g$) Production by Ruthenium(II) Complexes Containing Polyazaheterocyclic Ligands in Methanol and in Water. *Helv. Chim. Acta* **1996**, *79*, 1222–1238.
(25) Orellana, G.; Jiménez-Hernández, M. E.; García-Fresnadillo, D. Spanish Patent 2226 576.
(26) Xavier, M. P.; García-Fresnadillo, D.; Moreno-Bondi, M. C.; Orellana, G. Oxygen Sensing in Non-Aqueous Media Using Porous Glass with Covalently Bound Luminiscent Ru(II) Complexes. *Anal. Chem.* **1998**, *70*, 5184–5189.
(27) García-Fresnadillo, D.; Marazuela, M. D.; Moreno-Bondi, M. C.; Orellana, G. Luminescent Nafion Membranes Dyed with Ruthenium(II) Complexes as Sensing Materials for Dissolved Oxygen. *Langmuir* **1999**, *15*, 6451–6459.
(28) Bandala, E. R.; Arancibia-Bulnes, C. A.; Orozco, S. L.; Estrada, C. A. Solar Photoreactors Comparison Based on Oxalic Acid Photocatalytic Degradation. *Solar Energy* **2004**, *77*, 503–512.
(29) Malato, S.; Blanco, J.; Maldonado, M. I.; Fernández, P.; Alarcón, D.; Collares-Pereira, M.; Farinha, J.; Correia, J. Engineering of Solar Photocatalytic Collectors. *Solar Energy* **2004**, *77*, 513–524.
(30) Kalogirou, S. A. Solar Thermal Collectors and Applications. *Prog. Energy Combust. Sci.* **2004**, *30*, 231–295.
(31) Villén, L.; Manjón, F.; García-Fresnadillo, D.; Orellana, G. Solar Reactor for Water Disinfection by Sensitised Singlet Oxygen Production in Heterogeneus Medium. *Appl. Catal., B* **2006**, *69*, 1–9.
(32) (a) Chaves, J.; Collares-Pereira, M. New CPC Solar Collector for Planar Absorbers Immersed in Dielectrics. Application to the Treatment of Contaminated Water. *J. Sol. Energy. Eng.* **2007**, *129*, 16–21. (b) Collares-Pereira, M.; Correia de Oliveira, J. Portuguese Patent 102 938.
(33) ASTM G173–03 Reference Spectra; Solar Spectral Irradiance: Air Mass 1.5; EEUU, 2003. http://rredc.nrel.gov/solar/spectra/am1.5/ (accessed Oct 2007).
(34) Iqbal, M. *An Introduction to Solar Radiation*; Academic Press: Ontario, 1983
(35) Verlhac, J. B.; Gaudemer, A.; Kraljic, I. Water-Soluble Porphyrins and Metalloporphyrins as Photosensitizers in Aerated Aqueous Solutions. I. Detection and Determination of Quantum Yield of Formation of Singlet Oxygen. *Nouv. J. Chim.* **1984**, *8*, 401–406.
(36) Porter, G. B.; Sparks, R. H. Photoracemization of Ru(bipyridine)$_3^{2+}$. *J. Photochem.* **1980**, *13*, 123–131.
(37) Adelt, M.; Devenney, M.; Meyer, T. J.; Thompson, D. W.; Treadway, J. A. Ruthenium(II) MLCT Excited States. Stabilization toward Ligand Loss in Rigid Media. *Inorg. Chem.* **1998**, *37*, 2616–2617.
(38) Hartmann, P.; Leiner, M. J. P.; Kohlbacher, P. Photobleaching of a Ruthenium Complex in Polymers Used for Oxygen Optodes and Its Inhibition by Singlet Oxygen Quenchers. *Sens. Actuators, B* **1998**, *51*, 196–202.
(39) Vaidyalingam, A.; Dutta, P. K. Analysis of the Photodecomposition Products of Ru(bpy)$_3^{2+}$ in Various Buffers and Upon Zeolite Encapsulation. *Anal. Chem.* **2000**, *72*, 5219–5224.
(40) Fuller, Z. J.; Bare, W. D.; Kneas, K. A.; Demas, J. N.; DeGraff, B. A. Photostability of Luminescent Ruthenium(II) Complexes in Polymers and in Solution. *Anal. Chem.* **2003**, *75*, 2670–2677.
(41) Durham, B.; Caspar, J. V.; Nagle, J. K.; Meyer, T. J. Photochemistry of Ru(bpy)$_3^{2+}$. *J. Am. Chem. Soc.* **1982**, *104*, 4803–4810.
(42) Brandrup, J.; Immergut, E. H. *Polymer Handbook*, 3rd ed.; Wiley: New York, 1989.
(43) See: Cellon: CulturSil. www.cellon.lu/cultursil/cultursil.htm (accessed Oct 2007).
(44) Shimizu, O.; Watanabe, J.; Naito, S. Absolute Quantum Yields and Lifetimes of Photosensitized Phosphorescence of Singlet Oxygen O_2 ($^1\Delta_g$) in Air-Saturated Aqueous and Organic Solutions of Phenalenone. *Chem. Lett.* **1999**, 67–68.
(45) Fux, C. A.; Shirtliff, M.; Stoodley, P.; Costerton, J. W. Can Reference Laboratory Strains Mirror 'Real-World' Pathogenesis? *Trends Microbiol.* **2005**, *13*, 58–63.
(46) Navntoft, C.; Araujo, P.; Litter, M. I.; Apella, M. C.; Fernández, D.; Puchulu, M. E.; Hidalgo, M. V.; Blesa, M. A. Field Tests of the Solar Water Detoxification SOLWATER Reactor in Los Pereyra, Tucumán, Argentina. *J. Solar Energy Eng.* **2007**, *129*, 127–134.

ES071762Y